

Coordination Chemistry of Silver(I) with the Nitrogen-Bridged Ligands $(C_6H_5)_2PN(H)P(C_6H_5)_2$ and $(C_6H_5)_2PN(CH_3)P(C_6H_5)_2$: The Effect of Alkylating the Nitrogen Bridge on Ligand Bridging versus Chelating Behavior

E. J. Sekabunga, Michele L. Smith, T. R. Webb, and W. E. Hill*

Department of Chemistry, Auburn University, Auburn, Alabama 36849

Received June 21, 2001

The coordination chemistry of silver(I) with the nitrogen-bridged ligands $(C_6H_5)_2PN(R)P(C_6H_5)_2$ [$R = H$ (dppa); $R = CH_3$ (dppma)] has been investigated by ^{31}P NMR and electrospray mass spectrometry (ESMS). Species observed by ^{31}P NMR include $Ag_2(\mu\text{-dppa})_2^{2+}$, $Ag_2(\mu\text{-dppa})_2^{2+}$, $Ag_2(\mu\text{-dppa})_3^{2+}$, $Ag_2(\mu\text{-dppma})_2^{2+}$, $Ag_2(\mu\text{-dppma})_2^{2+}$, and $Ag(\eta^2\text{-dppma})_2^+$. Species observed by ESMS at low cone voltages were $Ag_2(dppa)_2^{2+}$, $Ag_2(dppa)_3^{2+}$, $Ag_2(dppma)_2^{2+}$, and $Ag(dppma)_2^+$. $(C_6H_5)_2PN(CH_3)P(C_6H_5)_2$ showed a strong tendency to chelate, while $(C_6H_5)_2PN(H)P(C_6H_5)_2$ preferred to bridge. Differences in the bridging versus chelating behavior of the ligands are assigned to the Thorpe–Ingold effect, where the methyl group on nitrogen sterically interacts with the phenyl groups on phosphorus. The crystal structure of the three-coordinate dinuclear silver(I) complex $\{Ag_2[(C_6H_5)_2PN(H)P(C_6H_5)_2]_3\}(BF_4)_2$ has been determined. Bond distances include $Ag\text{--}Ag = 2.812(1)$ Å, $Ag(1)\text{--}P(av) = 2.492(3)$ Å, and $Ag(2)\text{--}P(av) = 2.509(3)$ Å. The compound crystallizes in the monoclinic space group Cc at 294 K, with $a = 18.102(4)$ Å, $Z = 4$, $V = 7261(3)$ Å³, $R = 0.0503$, and $R_w = 0.0670$.

Introduction

The coordination chemistry of the hydrocarbon backbone bisphosphine ligand $Ph_2PCH_2PPh_2$ (dppm) has been widely studied and has shown great versatility as a ligand.¹ It exhibits a great ability to bridge metal centers in the μ -bonding mode, forming bi-^{1,2} and polynuclear complexes, the latter formed in the presence of a suitable capping ligand.³ Chelating behavior, i.e., the η^2 -bonding mode, has also been commonly observed,^{1,4} and some complexes with the ligand in the η^1 -bonding mode have also been reported.^{1,5}

The four-membered chelate rings formed by dppm are known to be highly strained,¹ though several reports of them have been made in the literature. These complexes have

typically been reported in square planar and octahedral coordination environments. The ability to form relatively stable four-membered chelate rings has been shown to give catalysts that are superior to those of larger rings.⁶

Replacement of the methylene protons with R groups ($R = \text{alkyl}$) has long been known to favor cyclization in organic chemistry (the Thorpe–Ingold and *gem*-dialkyl effects; the former refers to an angle change on substitution, while the latter refers to acceleration of the cyclization).⁷ In bisphosphine–metal coordination chemistry, substitution by methyl groups for hydrogen at the methylene carbon of dppm to

* To whom correspondence should be addressed. E-mail: hillwil@mail.auburn.edu.

- (1) (a) Chaudret, B.; Delavaux, B.; Poilblanc, R. *Coord. Chem. Rev.* **1988**, *86*, 191. (b) Haiduc, I.; Silaghi-Dimitrescu, I. *Coord. Chem. Rev.* **1986**, *74*, 127. (c) Puddephatt, R. J. *Chem. Soc. Rev.* **1983**, 99.
- (2) (a) Benson, J. W.; Keiter, E. A.; Keiter, R. L. *J. Organomet. Chem.* **1995**, *495*, 77. (b) Jacobsen, G. B.; Shaw, B. L.; Thornton-Pett, M. J. *Chem. Soc., Dalton Trans.* **1987**, 1509, and references therein. (c) Jacobsen, G. B.; Shaw, B. L.; Thornton-Pett, M. J. *Chem. Soc., Dalton Trans.* **1987**, 1489, and references therein.
- (3) Bera, J. K.; Nethaji, M.; Samuelson, A. G. *Inorg. Chem.* **1999**, *38*, 218.

- (4) (a) Mishra, A.; Agarwala, U. C. *Inorg. Chim. Acta* **1990**, *170*, 209. (b) Lindsay, C. H.; Benner, L. S.; Balch, L. *Inorg. Chem.* **1980**, *19*, 3505.
- (5) (a) Carriedo, G. A.; Carmen Crespo, M.; Diaz, C.; Riera, V. J. *Organomet. Chem.* **1990**, *397*, 309. (b) Canno, M.; Campo, J. A.; Ovejero, P.; Heras, J. V. *Inorg. Chim. Acta* **1990**, *170*, 139. (c) Canno, M.; Campo, J. A.; Perez-Garcia, V.; Gutierrez-Puebla, E.; Alvarez-Ibarra, C. *J. Organomet. Chem.* **1990**, *382*, 397.
- (6) (a) Dossett, S. J.; Gillon, A.; Orpen, A. G.; Fleming, J. S.; Pringle, P. G.; Wass, D. F.; Jones, M. D. *Chem. Commun.* **2001**, 699. (b) Angelici, R. J. *Acc. Chem. Res.* **1995**, *28*, 51, and references therein.
- (7) (a) Shaw, B. L. *J. Organomet. Chem.* **1980**, *200*, 307. (b) Beesley, R. M.; Ingold, C. K.; Thorpe, J. F. *J. Chem. Soc.* **1915**, 107, 1080. (c) Cope, A. C.; Friedrich, E. C. *J. Am. Chem. Soc.* **1968**, *90*, 909. (d) Shaw, B. L. *J. Am. Chem. Soc.* **1975**, *97*, 3856. (e) Jung, M. E.; Gervey, J. J. *Am. Chem. Soc.* **1991**, *113*, 224.

give 2,2-bis(diphenylphosphino)propane results in the ligand having a significantly greater propensity to form stable four-membered chelate rings than dpmm.⁸ Replacement of one methylene hydrogen on dpmm by a methyl group to give 1,1-bis(diphenylphosphino)ethane (1,1-dppe) also results in a ligand with chelating properties much like the well-known chelating ligand dppe.⁹

The coordination chemistry of the nitrogen-containing backbone bisphosphine ligand bis(diphenylphosphino)amine, Ph₂PNHPPH₂ (dppa; isoelectronic with dpmm), and its alkylated analogues, primarily bis(diphenylphosphino)methylamine, Ph₂PN(Me)PPh₂ (dppma), has received increasing attention, summarized in three excellent review articles.¹⁰ Dppa's bridging versus chelating behavior viz-a-viz dpmm is still a matter of contention, and there have been differing opinions as to which ligand is better for the different bonding modes.¹¹ Dppa has further been cited as especially attractive for metal coordination because the greater acidity of its N–H proton over the methylene protons of dpmm has been found to promote functionalization reactions on the ligand backbone.¹² In a fashion analogous to the dimethylation of the methylene bridge of dpmm and its effect on chelation ability, it has been found that methylating the N–H group of dppa to give dppma gives superior chelation (over dppa) in the square-planar platinum(II) complexes.¹³

We report a ³¹P{¹H} NMR and an electrospray mass spectrometric (ESMS) investigation of the effect of alkylation at the nitrogen bridge on the coordination chemistry of dppa and dppma with Ag(I). Ag(I) was chosen as the metal for coordination because it forms linear, triangular, and tetrahedral complexes and the magnitudes of the ¹J_{Ag–P} coupling constants have been related to the geometry.¹⁴ Furthermore there are few reports of four-membered chelate rings in the tetrahedral environment.

We also report the crystal and molecular structure of the dinuclear silver, triple bis-phosphine bridged cation [Ag₂-dppa₃]²⁺.

Results and Discussion

The range of Ag(I) complexes with the non-coordinating BF₄ counteranion produced in solution by the ligands dppa and dppma was investigated in solution at different stoichi-

ometries, i.e., ligand to metal concentration (C_L/C_M) ratios by variable-temperature ³¹P{¹H} NMR and ESMS.

Using the silver–phosphorus coupling constants ¹J(Ag–³¹P) obtained in the variable temperature ³¹P{¹H} NMR study of the various silver–bisphosphine systems in situ, the Ag–(I) coordination numbers were identified. In some cases in this study the ¹⁰⁷Ag–³¹P and ¹⁰⁹Ag–³¹P splittings were not resolved before solubility problems set in. Based on the ¹J(Ag–³¹P) values observed and those proposed previously,¹⁴ i.e., 500, 316–321, and 224–230 Hz, for two-, three-, and four-coordinate silver(I), respectively, silver(I) here existed in solution in various coordination numbers ranging from 1 to 4 with the ligands at temperatures of 295 K to as low, where solubility permitted, as 213 K. The coordination of the ligands to silver resulted, in all cases, in a downfield shift, as is the general case in the coordination of phosphines.¹⁵

ESMS involves the gentle transfer of ions from solution, with little or no fragmentation, to the gas phase followed by conventional mass analysis methods.¹⁶ ESMS has increasingly found utilization in the analysis of inorganic and organometallic complexes in solution.¹⁷ The electrospray mass spectral peaks are identified from the most intense peak in the observed isotopic mass distribution. Silver with its two isotopes ¹⁰⁷Ag and ¹⁰⁹Ag of almost equal abundance (52 and 48%, respectively) eases the elucidation of the number of silver atoms contained in the complexes. The experimental and calculated isotopic mass distributions were in excellent agreement.

Variable-Temperature ³¹P{¹H} NMR Studies of dppa and AgBF₄. From results of the variable-temperature study of silver(I) with dppa given in Table 1, increasing the C_L/C_M ratio led to higher coordination numbers as evidenced by the decreasing ¹J(Ag–³¹P) values observed. Variations in C_L/C_M ratios form one- (¹J(Ag–³¹P), ca. 740–796 Hz), two- (¹J(Ag–³¹P), 523–576 Hz), and three-coordinate (¹J(Ag–³¹P), ca. 326–354 Hz) complexes with dppa. Complexes atypical in the Muetterties and Alegrianti scheme¹⁴ are those with ¹J(Ag–³¹P) values in the 740–796 Hz range, and the complex with dppa that has a ¹J(Ag–P) of 171 Hz. Complexes with ¹J(Ag–P) > 700 were observed at low C_L/C_M ratios and were assigned as a one-coordinate¹⁸ silver(I) complex, [Ag₂(μ-dppa)]²⁺, while the latter observed at a C_L/C_M ratio = 4.0, and resolved at low temperature, showed a silver–phosphorus coupling identical to that reported by

- (8) (a) Barkley, J. V.; Ellis, M.; Higgins, S. J.; McCart, M. K. *Organometallics* **1998**, *17*, 1725. (b) Barkley, J. V.; Grimshaw, J. C.; Higgins, S. J.; Hoare, P. B.; McCart, M. K.; Smith, A. K. *J. Chem. Soc., Dalton Trans.* **1995**, 2901.
- (9) Vila, J. M.; Gayoso, M.; Torres, M. L.; Fernandez, J. J.; Fernandez, A.; Ortigueira, J. M.; Bailey, N. A.; Adams, H. *J. Organomet. Chem.* **1996**, *511*, 129.
- (10) (a) Bhattacharyya, P.; Woollins, D. J. *Polyhedron* **1995**, *14*, 3367, and references therein. (b) Balakrishna, M. S.; Reddy, S. V.; Krishnamurthy, S. S.; Nixon, J. F.; Burckett St. Laurent, J. C. T. R. *Coord. Chem. Rev.* **1994**, *129*, 1, and references therein. (c) Witt, M.; Roesky, H. W. *Chem. Rev.* **1994**, *94*, 1163, and references therein.
- (11) Bachert, I.; Braunstein, P.; McCart, M. K.; Fabrizi de Biani, F.; Laschi, F.; Zanello, P.; Kickelbick, G.; Schubert, U. *J. Organomet. Chem.* **1999**, *573*, 47, and references therein.
- (12) Bachert, I.; Bartussek, I.; Braunstein, P.; Guillon, E.; Rose, J.; Kickelbick, G. *J. Organomet. Chem.* **1999**, *580*, 257.
- (13) Browning, S. C.; Farrar, D. H. *J. Chem. Soc., Dalton Trans.* **1995**, 521.
- (14) Muetterties, E. L.; Alegrianti, C. W. *J. Am. Chem. Soc.* **1970**, *92*, 4114.

- (15) Garrou, P. E. *Chem. Rev.* **1981**, *81*, 229.
- (16) (a) Dole, M.; Mack, L. L.; Hines, R. L.; Mobley, R. C.; Ferguson, L. D.; Alice, M. B. *J. Chem. Phys.* **1968**, *49*, 2240. (b) Yamashita, M.; Fenn, J. B. *J. Phys. Chem.* **1984**, *88*, 4451. (c) Whitehouse, C. M.; Dreyer, R. N.; Yamashita, M. *Anal. Chem.* **1985**, *57*, 675. (d) Kebarle, P.; Tang, L. *Anal. Chem.* **1993**, *65*, 972.
- (17) (a) Hopp, C. E. C. A.; Saulys, D. A.; Gaines, D. F. *Inorg. Chem.* **1995**, *34*, 1977. (b) Ahmed, I.; Bond, A. M.; Colton, R.; Jurcevic, M.; Traeger, J. C.; Walter, J. N. *J. Organomet. Chem.* **1993**, *447*, 59. (c) Colton, R.; James, B. D.; Potter, I. D.; Traeger, J. C. *Inorg. Chem.* **1993**, *32*, 2626. (d) Bond, A. M.; Colton, R.; D'Agostino, A.; Harvey, J.; Traeger, J. C. *Inorg. Chem.* **1993**, *32*, 3952. (e) Aliprantis, A. O.; Canary, J. W. *J. Am. Chem. Soc.* **1994**, *116*, 6985.
- (18) (a) Attar, S.; Alcock, N. W.; Bowmaker, G. A.; Frye, J. S.; Bearden, W. H.; Nelson, J. H. *Inorg. Chem.* **1991**, *30*, 4166, and references therein. (b) van der Ploeg, A. F. M. J.; van Koten, G.; Spek, A. L. *Inorg. Chem.* **1979**, *18*, 1052.

Table 1. Variable-Temperature ³¹P{¹H} NMR Study of AgBF₄ and Bis(diphenylphosphino)amine (dppa)^a

C _L /C _M ratio	δ(³¹ P), ^b ppm	¹ J(Ag–P), Hz	rel area	temp, K	Ag ⁺ CN ^c	assigned struct
0.5	66.3	740	0.75	263	1	[Ag ₂ (μ-L)] ₂
	63.4	527 ^d	0.25	263	2	[Ag ₂ (μ-L) ₂] ²⁺
	66.6	796	0.58	238	1	[Ag ₂ (μ-L)] ²⁺
	63.4	527 ^d	0.42	238	2	[Ag ₂ (μ-L) ₂] ²⁺
	66.3	779	0.53	228	1	[Ag ₂ (μ-L)] ²⁺
1	63.3	528 ^d	0.47	228	2	[Ag ₂ (μ-L) ₂] ²⁺
	63.9	528 ^d	1	295	2	[Ag ₂ (μ-L) ₂] ²⁺
1.25	63.5	523 ^d	0.84	273	2	[Ag ₂ (μ-L) ₂] ²⁺
	56.4	327 ^d	0.16	273	3	[Ag ₂ (μ-L) ₃] ²⁺
	63.5	523 ^d	0.82	253	2	[Ag ₂ (μ-L) ₂] ²⁺
	56.1	327 ^d	0.18	253	3	[Ag ₂ (μ-L) ₃] ²⁺
	63.5	523 ^d	0.81	233	2	[Ag ₂ (μ-L) ₂] ²⁺
	56.2	326 ^d	0.19	233	3	[Ag ₂ (μ-L) ₃] ²⁺
	63.6	576	0.05	295	2	[Ag ₂ (μ-L) ₂] ²⁺
1.5	56.5	354	0.95	295	3	[Ag ₂ (μ-L) ₃] ²⁺
	63.2	548	0.09	253	2	[Ag ₂ (μ-L) ₂] ²⁺
	56.5	349	0.91	253	3	[Ag ₂ (μ-L) ₃] ²⁺
	56.6	349	0.67	253	3	[Ag ₂ (μ-L) ₃] ²⁺
2	53	461	0.05	253		
	22.5	e	0.28	253		
4	54.3	f	0.09	253		
	51.5	171	0.47	253	3	[Ag(η ¹ -L) ₃] ⁺
	26.9	e	0.05	253		
	21.7	e	0.28	253		

^a (0.5–0.8) × 10^{−3} M (based on expected complex; see Experimental Section) solutions in methylene chloride, CDCl₃, and acetone (see Experimental Section). ^b Relative to 85% H₃PO₄. ^c Ag⁺ coordination number discerned from ¹J(Ag–P) value. ^d ¹J(¹⁰⁷Ag–P). Spectra resolved well enough to discern this coupling. ^e Single sharp peak ^f Broad peak

Peringer and co-workers,¹⁹ for [Ag(η¹-dppm)₃]⁺, and was thus assigned similarly.

The ³¹P NMR spectrum of an isolated sample at 253 K from the C_L/C_M ratio = 1.0 showed the second-order effects of long-range coupling and resolution of ¹⁰⁷Ag–P and ¹⁰⁹-Ag–P coupling (¹J(¹⁰⁷Ag–P), 524 Hz; ¹J(¹⁰⁹Ag–P), 603 Hz; δ(³¹P), 63.5 ppm). The spectrum along with a simulated spectrum led to the assignment as the dinuclear doubly bisphosphine-bridged complex [Ag₂(μ-dppa)₂]²⁺. This dinuclear, double-bridged framework has been reported in the solid state for analogue dppm.^{20,21}

The three-coordinate complex (¹J(¹⁰⁷Ag–P), 326 Hz; δ-⁽³¹P), 56.5 ppm) was assigned the manxane-like binuclear triply bridged framework [Ag₂(μ-dppa)₃]²⁺ as its dmpm (bis-(dimethylphosphino)methane) and dppm analogues were in solution using variable-temperature ³¹P NMR^{19,22} and found in the solid-state for dppm²¹ and in agreement with its solid-state structure found in this work. Four-coordinate silver(I) was not observed with dppa.

ESMS of dppa and AgBF₄. Table 2 summarizes the species observed in ESMS for the dppa and AgBF₄ mixtures at a cone voltage of 20 V. The dppa and AgBF₄ mixture, C_L/C_M = 0.5, in a 50 vol % acetonitrile/water solution at a cone voltage of 20 V showed no significant peaks below *m/z* = 300. The mass spectrum was dominated by the peak at *m/z* = 493, which was assigned to the binuclear [Ag₂-

Table 2. Electrospray Mass Spectral Results at a Cone Voltage of 20 V for Solutions of AgBF₄ and Dppa at Various Ligand to Metal Ratios^a

C _L /C _M	[Ag ₂ L ₂] ²⁺	[Ag ₂ L ₃] ²⁺	[AgL ₂] ²⁺	others ^b
0.5	493 (100)			688 (<10) 1023 (<10)
				1023 (<10)
1.0	493 (100)	685.5 (34)		1023 (<10)
1.5	493 (8)	685.5 (100)		1370 (<10) 1078 (<10) 1023 (<10)
				1447 (<10)
4.0		685.5 (100)	879 (<10)	1406 (<10) 1370 (<10)

^a Reported as *m/z* (relative intensity); solvent, CH₃CN/H₂O, 50:50 vol %; concentration of silver, 1 × 10^{−3} M. ^b 688 (<10), Ag₂LBF₄⁺; 1023 (<10), Ag₂L₂(H₂O)OH⁺; 1078 (<10), unassigned; 1370 (<10), Ag₂L₂(L–H)⁺; 1406 (<10), Ag₂L₃(H₂O)OH⁺; 1447 (<10), Ag₂L₃(CH₃CN)(H₂O)OH⁺.

(dppa)₂]²⁺ complex, inferred from the experimental and calculated isotopic patterns. Minor (base peak intensity, bpi < 10%) peaks and their assignments are listed in Table 2. All species observed at this voltage were derived from the complexes [Ag₂(dppa)]²⁺ and [Ag₂(dppa)₂]²⁺. These were the same two complexes (for the same ligand:metal ratio) observed in solution by ³¹P NMR.

At a cone voltage of 35 V an additional peak *m/z* = 985 (53%) assigned as [Ag₂(dppa)(dppa-H)]⁺ (where dppa-H is the deprotonated dppa to give an amide bridge) appeared. By a cone voltage of 65 V the amide species *m/z* = 985 [Ag₂(dppa)(dppa-H)]⁺ was the dominant peak. At cone voltages of 65–110 V, a host of solvent cluster and fragmentation species was observed with the [Ag(dppa)]¹⁺ fragment dominant at 110 V.

The assignment for the peak at *m/z* = 985 merits some further consideration. A *m/z* = 985 peak could have been the singly charged [Ag₂(dppa)₂]⁺ complex in which one silver atom was reduced, i.e., from Ag(I) to Ag(0). This would render the total charge of +1 on the complex. This would

(19) Obendorf, D.; Probst, M.; Peringer, P.; Falk, H.; Muller, N. *J. Chem. Soc., Dalton Trans.* **1988**, 1709.

(20) (a) Ho, D. M.; Bau, R. *Inorg. Chem.* **1983**, 22, 4073. (b) Tiekink, E. T. *Acta Crystallogr.* **1990**, C46, 235. (c) Sekabunga, E. J.; Hill, W. E. Unpublished work.

(21) Hong, M.; Wu, D.; Liu, H.; Mak, T. C. W.; Zhou, Z.; Wu, D.; Li, S. *Polyhedron* **1997**, 16, 1957.

(22) Dean, P. A. W.; Vittal, J. J.; Srivastava, R. S. *Can. J. Chem.* **1987**, 65, 2628.

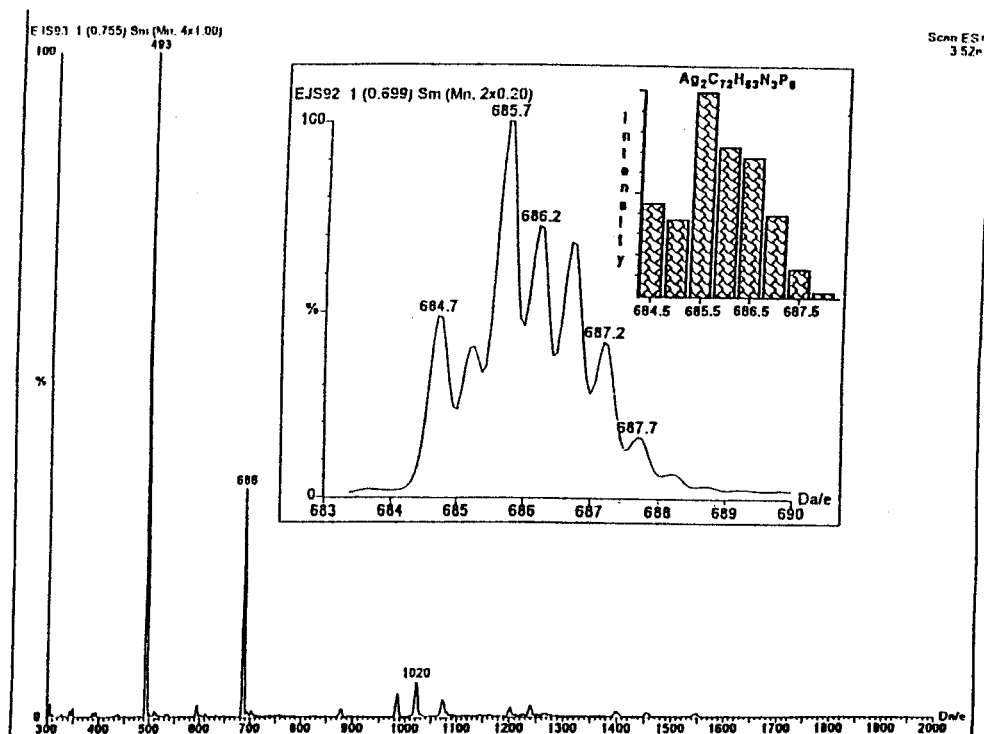


Figure 1. Electrospray mass spectrum of a DPPA/AgBF₄ mixture, $C_L/C_M = 1.0$, at a sampling cone voltage of 20 V.

be consistent with what has been reported to occur in FAB (fast atom bombardment) mass spectroscopy, i.e., that FAB provides an essentially reducing environment.²³ Reports of reduction occurring during electrospray mass spectrometry have been made by Curtis et al.,²⁴ for Eu(III) to Eu(II), and Allen et al.,²⁵ for Cu(II) to Cu(I) and Co(III) to (II). The latter group reported increased reduction with increasing cone voltage. A comparison here of the experimental isotopic mass distribution with that calculated for the reduced species and the deprotonated species showed a match with the latter species. Thus, at higher collisional energies (i.e., at more energetic collisions with solvent molecules), the $[\text{Ag}_2(\text{dppa})_2]^{2+}$ complex lost a proton to yield the amide $[\text{Ag}_2(\text{dppa})(\text{dppa-H})]^{2+}$. This phenomenon was observed for the $[\text{Ag}_2(\text{dppm})_2]^{2+}$ complex,^{20c} where the onset of the acidity occurred at greater collisional energies in the ion source (cone voltages of ca. 65 vs 35 V observed here). The qualitative implication of this comparison is that the amine proton of dppa is more acidic than the methylene proton of dppm, a well-accepted fact.

Thus, as collisional energies increased, the $[\text{Ag}_2(\text{dppa})_2]^{2+}$ complex was transformed into the more stable amide complex $[\text{Ag}_2(\text{dppa})(\text{dppa-H})]^+$, which has ionic interactions in addition to the coordination bonds holding the silver and phosphorus together. Appearance of this phenomenon can be taken as a sign of the onset of fragmentation of the silver-bisphosphine complexes and thus a signal that electrospray

mass spectrometry is no longer a reliable mirror of the solution species.

The electrospray mass spectrum of an aqueous acetonitrile solution of a dppa and AgBF₄ mixture ($C_L/C_M = 1.0$) at a cone voltage of 20 V is shown in Figure 1, Table 2. The dominant peak, $m/z = 493$ was assigned as $[\text{Ag}_2(\text{dppa})_2]^{2+}$, a major peak at $m/z = 686$ (displayed with an insert of the experimental and calculated isotopic mass distributions) assigned as $[\text{Ag}_2(\text{dppa})_3]^{2+}$.

Figure 2 shows the experimental isotopic mass distributions of peak $m/z = 493$ in the $C_L/C_M = 1.0$ mixture from sampling cone voltages of 20, 45, and 50 V. At 20 V the experimental isotopic mass distribution agreed closely with that calculated for a binuclear species. By a cone voltage of 45 V there was a clear transition from a binuclear species to a mononuclear species. By a cone voltage of 50 V, the mononuclear fragment was predominant, as judged by close agreement of the observed and calculated isotopic mass distributions. Thus, it was determined that cone voltages from 20 to 30 V caused minimum fragmentation and were the best complement to NMR studies.

At a cone voltage of 20 V the species observed were, or were derivatives of, the complexes $[\text{Ag}_2(\text{dppa})_2]^{2+}$ and $[\text{Ag}_2(\text{dppa})_3]^{2+}$, species observed in ³¹P NMR in this work. At 35 V the amide complex $[\text{Ag}_2(\text{dppa})(\text{dppa-H})]^+$ was observed along with $[\text{Ag}(\text{dppa})_2]^+$. Both species were not observed by the ³¹P NMR studies and probably result from the onset of fragmentation in the ion source.

The species observed at cone voltages of 50 V and above are the result of fragmentation in the gas phase. To test this proposition, i.e., that these species are a result of gas-phase fragmentation, an excess of formic acid was added to the

- (23) Bignozzi, C. A.; Bortolini, O.; Curcuruto, O.; Hamdan, M. *Inorg. Chim. Acta* **1995**, 233, 113 and references therein.
 (24) Curtis, J. M.; Derrick, P. J.; Schnell, A.; Constantin, E.; Gallagher, R. T.; Chapman, J. R. *Inorg. Chim. Acta* **1992**, 201, 197.
 (25) Allen C. S.; Chuang, C. L.; Cornebise, M.; Canary, J. W. *Inorg. Chim. Acta* **1995**, 239, 29.

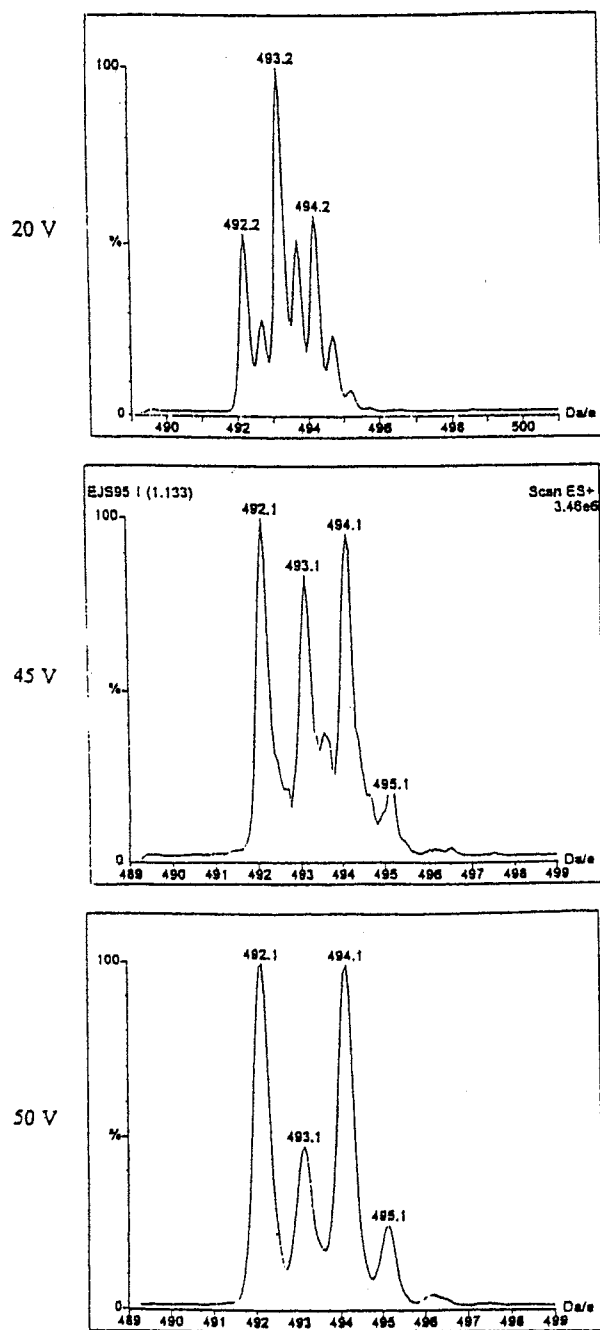


Figure 2. Fragmentation of $[\text{Ag}_2(\text{DPPA})_2]^{2+}$ in electrospray mass spectrometry monitored between sampling cone voltages of 20–50 V.

mixture to suppress any amide formation in solution. This acidified solution was then run at a cone voltage of 80 V, the cone voltage at which the amide $[\text{Ag}_2(\text{dppa})(\text{dppa-H})]^+$ showed maximum intensity. The result, in which there was no suppression of the amide peak at $m/z = 984$, clearly showed that this fragmentation, in the form of amide formation, was a gas-phase phenomenon, i.e., a case of gas-phase acidity.

The electrospray mass spectrum of an aqueous acetonitrile solution of dppa and AgBF_4 ($C_L/C_M = 1.5$) at a cone voltage of 20 V (Table 2) was dominated by the peak $m/z = 686$ assigned as $[\text{Ag}_2(\text{dppa})_3]^{2+}$; this was in agreement with the ^{31}P NMR results.

By a cone voltage of 35 V, the $[\text{Ag}_2(\text{dppa})_3]^{2+}$ complex still showed the dominant peak at $m/z = 686$ though appreciable amounts of the deprotonated complex was observed. Above cone voltages of 50 V, only fragmentation products were observed.

An aqueous acetonitrile solution of a dppa– AgBF_4 mixture ($C_L/C_M = 4.0$) at a cone voltage of 20 V was also investigated (Table 2). The aim of this was to have an excess of ligand and thus favor the possible formation of the bis-chelate $[\text{Ag}(\text{dppa})_2]^+$. The spectrum was dominated by the peak $m/z = 685$ assigned as $[\text{Ag}_2(\text{dppa})_3]^{2+}$.

Thus, the dominant complexes identified in solution by ESMS at conditions of minimum fragmentation, i.e., a cone voltage of 20 V, are $[\text{Ag}_2(\text{dppa})_2]^{2+}$ and $[\text{Ag}_2(\text{dppa})_3]^{2+}$ (Table 2).

Variable-Temperature ^{31}P NMR of dppma and AgBF_4 .

Three types of silver(I)–dppma complexes were observed in solution (Table 3), based on $^1J(^{107}\text{Ag}-^{31}\text{P})$ values, i.e., ca. 745, 524, and 221 Hz. These were identified as the one-, two-, and four-coordinate silver(I) complexes, respectively. Three-coordinate silver(I) complexes were not detected.

The one-coordinate silver(I) complex, $^1J(^{107}\text{Ag}-^{31}\text{P}) = 745$ Hz, $\delta(^{31}\text{P}) = 82.7$ ppm, was assigned¹⁸ the structure $[\text{Ag}_2(\mu\text{-dppma})_2]^{2+}$, while the two-coordinate complex, $^1J(^{107}\text{Ag}-^{31}\text{P}) = 524$ Hz, $\delta(^{31}\text{P}) = 81.5$ ppm, whose ^{31}P NMR spectra showed second-order coupling effects, was assigned the structure $[\text{Ag}_2(\mu\text{-dppma})_2]^{2+}$. The simulated spectra showed coupling constant values identical to those of $[\text{Ag}_2(\mu\text{-dppma})_2]^{2+}$. The four-coordinate silver(I) complex was assigned as the mononuclear bis-chelated $[\text{Ag}(\eta^2\text{-dppma})_2]^{2+}$, a framework observed previously with dppc.²⁶

ESMS of dppma and AgBF_4 . Table 4 summarizes the species observed in ESMS at cone voltage, 20 V for aqueous acetonitrile solutions of dppma and AgBF_4 mixtures ($C_L/C_M = 0.5\text{--}2$).

At $C_L/C_M = 0.5$, the mass spectra at the low fragmentation cone voltages of 20 and 35 V were dominated by the $m/z = 507$ peak assigned as $[\text{Ag}_2(\text{dppma})_2]^{2+}$ with lesser amounts of $[\text{Ag}_2(\text{dppma})_2(\text{BF}_4)]^+$, $m/z = 1101$ (Table 4). At a cone voltage of 50 V the fragment $[\text{Ag}(\text{dppma})]^+$, $m/z = 507$, became the base peak and $[\text{Ag}(\text{dppma})_2]^+$, $m/z = 907$ (31%), emerged as a significant peak. The latter species was considered here as a fragmentation product in the presence of the former. From a sampling cone voltage of 50–110 V the mass spectra were dominated by $[\text{Ag}(\text{dppma})]^+$ and $[\text{Ag}(\text{dppma})_2]^+$.

Noticeably absent here and indeed for all the ESMS studies with dppma was what is analogous to amide formation observed for the dppa complexes, i.e., the loss of the methyl group from dppma under harsh fragmentation conditions. This was in agreement with the well-established fact that the proton is a much better leaving group than the methyl group.

The $C_L/C_M = 1.0$ and 1.5 mixtures gave mass spectra that were essentially similar from the standpoint of species

(26) Berners Price, S. J.; Brevard, C.; Pagelot, A.; Sadler, P. J. *Inorg. Chem.* **1985**, *24*, 4278.

Table 3. Variable-Temperature $^{31}\text{P}\{^1\text{H}\}$ NMR Study of AgBF_4 and Bis(diphenylphosphino)methylamine (dppma)^a

C_L/C_M ratio	$\delta(\text{P}),^b$ ppm	$^1J(\text{Ag}-\text{P}),$ Hz	rel area	temp, K	AgI CN ^c	assigned struct
0.5	83.2	733	0.82	263	1	$[\text{Ag}_2(\mu\text{-L})]^{2+}$
	82	540	0.18	263	2	$[\text{Ag}_2(\mu\text{-L})_2]^{2+}$
	82.7	745 ^d	1	213	1	$[\text{Ag}_2(\mu\text{-L})]^{2+}$
1	81.5	524 ^d	1	295	2	$[\text{Ag}_2(\mu\text{-L})_2]^{2+}$
	81.5	524 ^d	1	213	2	$[\text{Ag}_2(\mu\text{-L})_2]^{2+}$
1.5	81.7	521 ^d	0.53	295	2	$[\text{Ag}_2(\mu\text{-L})_2]^{2+}$
	89.3	221 ^d	0.47	295	4	$[\text{Ag}(\eta^2\text{-L})_2]^+$
2	81.3	560	0.07	295	2	$[\text{Ag}_2(\mu\text{-L})_2]^{2+}$
	89.4	221 ^d	0.93	295	4	$[\text{Ag}(\eta^2\text{-L})_2]^+$

^a $(0.5-0.8) \times 10^{-3}$ M (based on expected complex; see Experimental Section) solutions in methylene chloride, CDCl_3 , and acetone (see Experimental Section). ^b Relative to 85% H_3PO_4 . ^c Ag^+ coordination number discerned from $^1J(\text{Ag}-\text{P})$ value. ^d $^1J(^{107}\text{Ag}-\text{P})$. Spectra resolved well enough to discern this coupling.

Table 4. Electrospray Mass Spectral Results at a Cone Voltage of 20 V for Solutions of AgBF_4 and Dppma at Various Ligand to Metal Ratios^a

C_L/C_M	$[\text{Ag}_2\text{L}_2]^{2+}$	$[\text{AgL}_2]^{2+}$	others ^b
0.5	507 (100)		1101 (<10)
1.0	507 (100)	907 (12)	1101 (16)
			1051 (<10)
1.5	507 (56)	907 (100)	637 (<10)
			1101 (<10)
			1051 (<10)
2.0		907 (100)	1448 (<10)

^a Reported as m/z (relative intensity); solvent, $\text{CH}_3\text{CN}/\text{H}_2\text{O}$, 50:50 vol %; concentration of silver, 1×10^{-3} M. ^b 637 (<10), unassigned; 1051 (<10), $\text{Ag}_2\text{L}_2(\text{H}_2\text{O})(\text{OH})^+$; 1101 (<10), $\text{Ag}_2\text{L}_2\text{BF}_4^+$; 1448 (<10), $\text{Ag}_2\text{L}_3(\text{H}_2\text{O})\text{OH}^+$.

observed. At $C_L/C_M = 1.0$ under mild conditions (sampling cone voltages of 20 and 35 V), $[\text{Ag}_2(\text{dppma})_2]^{2+}$ and its ionic cluster derivative $[\text{Ag}_2(\text{dppma})_2(\text{BF}_4)]^+$ dominated the spectra with minor amounts of $[\text{Ag}(\text{dppma})_2]^+$ present. At $C_L/C_M = 1.5$, under mild conditions, $[\text{Ag}(\text{dppma})_2]^+$ dominated the mass spectra, with lesser amounts of $[\text{Ag}_2(\text{dppma})_2]^{2+}$ present. An interesting feature of the mass spectra was the absence of $[\text{Ag}_2(\text{dppma})_3]^{2+}$ or any of its ionic cluster derivatives, which was in agreement with its absence in ^{31}P NMR.

The mass spectra of the $C_L/C_M = 2.0$ mixtures were dominated by the $m/z = 907$ peak assigned as $[\text{Ag}(\text{dppma})_2]^+$ from the mild conditions at cone voltages of 20 and 35 V up to the harsher fragmentation voltage of 80 V. The known fragmentation product $[\text{Ag}(\text{dppma})]^+$ appeared at 80 V.

The ESMS results are clearly seen to agree with those of the ^{31}P NMR solution studies at the softer ionization (low cone voltage) conditions, where the gas-phase fragmentation is minimal. Of possible interest here was the observation that those ligands which underwent deprotonation in their complexes under harsh fragmentation conditions in ESMS; i.e., dppm^{20c} and dppa were the ligands not seen to chelate to $\text{Ag}(\text{I})$ in solution by ^{31}P NMR. The complexes identified in solution by ESMS at conditions of minimum fragmentation, i.e., a cone voltage of 20 V, are $[\text{Ag}_2(\text{dppma})_2]^{2+}$ and $[\text{Ag}(\text{dppma})_2]^+$ (Table 4).

The ^{31}P NMR and ESMS evidence agree to the existence in solution at the different C_L/C_M ratios of the dppa complexes $[\text{Ag}_2(\mu\text{-dppa})]^{2+}$, $[\text{Ag}_2(\mu\text{-dppa})_2]^{2+}$, and $[\text{Ag}_2(\mu\text{-dppa})_3]^{2+}$. The dppma complexes discerned by both techniques are $[\text{Ag}_2(\mu\text{-dppma})_2]^{2+}$ and $[\text{Ag}(\eta^2\text{-dppma})_2]^{2+}$. The

intact complex $[\text{Ag}_2(\mu\text{-dppma})]^{2+}$ was not detected by ESMS. It is an interesting note that dppa like dppm^{20c} forms the dinuclear one-, two-, and three-coordinate complexes with silver(I). Dppma on the other hand forms the dinuclear one-, two-, and mononuclear four-coordinate complexes with silver(I) much like the two-carbon interdonor phosphorus backbone ligand, dppe.^{20c}

The nonformation of the mononuclear bis-chelated four-coordinate silver(I) complex, $[\text{Ag}(\text{dppm})_2]^+$, was explained as being due to ring strain.¹⁹ It was pointed out that dppm chelate rings show P–M–P or chelate bite angles generally ranging from 67 to 74°, this being much lower than the ideal tetrahedral angle of 109° and causing an excessive strain on the four-membered ring. The same may be said about dppa here.

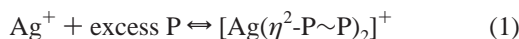
Further, an analogous observation where 2,2-bis(diphenylphosphino)propane (2,2-dppp) shows greater propensity to chelate than dppm in octahedral $\text{Ru}(\text{II})$ complexes has been reported in the literature.^{8b} This was attributed to the fact that complete replacement of hydrogen at the methylene carbon by the more bulky methyl groups would greatly enhance the stability of the four-membered chelate ring. This cyclization effect has been known in carbon ring chemistry for a number of years and is discussed as Thorpe–Ingold and *gem*-dialkyl effects.⁷

Since the nitrogen atom is smaller than the carbon atom, nitrogen chemistry should be significantly affected by methyl groups. This methyl group effect has been used to explain the cyclopalladation of dimethylbenzylamine,^{7a,c} chemistry that was not observed with benzylamine.^{7a,d} This methyl group effect was observed in the present study when comparing the coordination of dppa and dppma to $\text{Ag}(\text{I})$. The formation of the stable bis-chelated $[\text{Ag}(\text{dppma})_2]^{2+}$ of probable tetrahedral geometry in solution and the nonobservance for the analogous dppa case was thus attributed to a methyl group effect on the nitrogen backbone of dppma. This is not unlike the Thorpe–Ingold and *gem*-dialkyl effects known for carbon. This cyclization effect has steric origins. Two factors, an entropy factor and an enthalpy factor, have been identified as responsible for this alkyl effect.^{7c} Considering the two ligands dppa and dppma, the latter has more hindered rotation about the P–N bond due to the steric interaction of the methyl group on the backbone N and the phenyl groups on the P atoms. As a result, the loss of internal rotational entropy that occurs on chelation was less in dppma

than in dppa. The enthalpy factor arose from the fact that the increase in the number of gauche interactions that occur on chelation is less for dppma. This is because the methyl group in dppma increased the gauche interactions in the ligand over those in dppa. Indeed, a comparison of the Pt(II) coordination chemistry with dppa and dppma revealed that though both ligands form stable bis-chelated square-planar complexes with the metal, dppma was reported to be the superior chelator.¹³

Dppa, however, has been shown to chelate in the solid state and solution in the monochelate tetrahedral Cu(I) complexes [Cu(η^2 -dppa)(PPh₃)₂]⁺NO₃⁻ and [Cu(η^2 -dppa)(CN)PPh₃]^{27b}, where the chelate bite angles were 70.8 and 71.4°, respectively, a large deviation from the ideal. The P–N–P angles are 109.3 and 107.9°, respectively, a considerable distortion from the ideal trigonal-planar angle expected at the sp²-hybridized nitrogen and the angle of 118.9° observed in the free ligand.²⁸

From this work it appears that Ag(I) in its highest coordination numbers with these short-backbone bidentate ligands was either three-coordinate (i.e., the dinuclear triply bridged [Ag₂(P~P)₃]²⁺) or four-coordinate (as the bis-chelated mononuclear complex [Ag(P~P)₂]⁺) but did not show both coordination modes for a ligand. Dppm^{20c} and dppa form the former complex while dppe^{20c} and dppma form the bis-chelate. One can envisage the following alternative coordination schemes:



The chelation (i) was dominant if ring strain could be minimized, either by the formation of a five-membered ring as with dppe or by a Thorpe–Ingold effect with dppma. In cases where the ring strain was untenable, i.e., dppa and dppm, (ii) the favored chelation was overcome and the dinuclear triply bridged ring formation took precedence.

Structure of [Ag₂(dppa)₃](BF₄)₂·H₂O. The crystal structure of the cationic complex [Ag₂(dppa)₃]²⁺ from [Ag₂(dppa)₃](BF₄)₂·H₂O is shown in Figure 3. The complex consists of two essentially trigonal-planar AgP₃ units in a nearly eclipsed configuration that are bridged by P–N–P moieties of the dppa ligands in a paddlewheel arrangement about the two metal centers with no imposed symmetry but with rough D₃ symmetry for the cations. This is illustrated in Figure 3b. A twist about the barrel axis of 22(3)° was observed.

This “manxane”-like structure was deduced previously in solution by ³¹P NMR for the [Ag₂(μ -dppm)₃]²⁺ cation¹⁹ and the [Ag₂(μ -dmpm)₂]²⁺ cation.²² This is also in agreement with the ³¹P NMR and ESMS structural assignment in this work, and one of a few reported crystallographic determinations of a binuclear silver triply bis-phosphine bridged

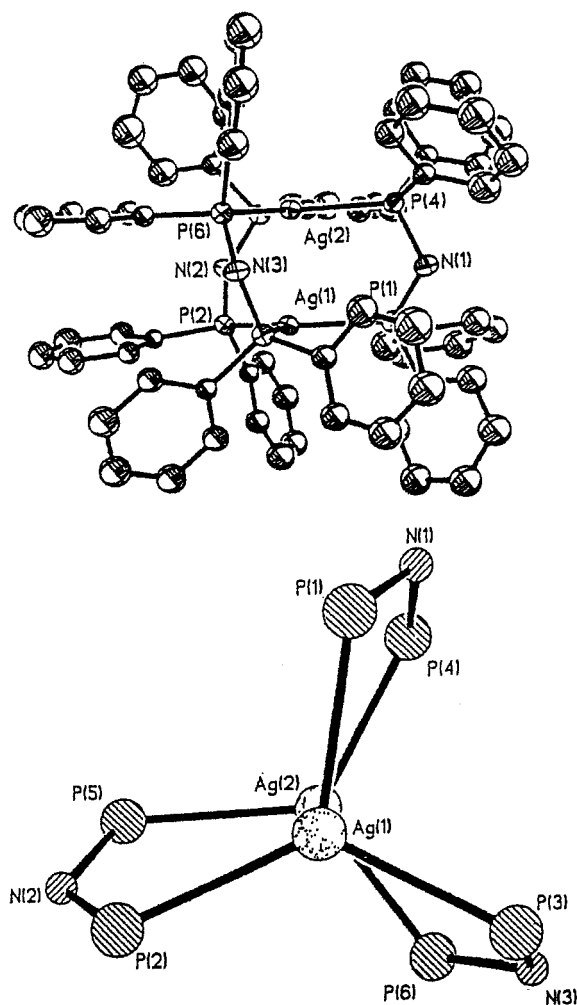


Figure 3. (a, top) ORTEP diagram of [Ag₂(DPPA)₃]²⁺. (b, bottom) ORTEP diagram of the core of [Ag₂(DPPA)₃]²⁺ (view along the Ag...Ag axis).

complex. Two others are with dppm and 2,6-bis(diphenylphosphino)pyridine.^{21,29} Crystal structures of a similar structural type, [M₂(μ -P~P)₃]ⁿ⁺, however, have also been reported for Au(I) with P~P = 2,6-bis(diphenylphosphino)pyridine³⁰ and bis(dimethylphosphino)methane, dmpm,³¹ Pd(0) with P(OPh)₂N(Me)P(OPh)₂³² and dppm,³³ and Pt(II) with dppm.³⁴

The P–Ag–P angles (Table 5) range between 109.6(1) and 127.1(1)°; the average value about each silver atom is 120.0°, showing the trigonal character. This variation differs from the [Ag₂(μ -dppm)₃]²⁺ cation where each silver was reported in exactly ideal trigonal-planar geometry.²¹ This average P–Ag–P angle is comparable to those observed in

(27) (a) Ellermann, J.; Knoch, F. A.; Meier, K. J.; Moll, M. *J. Organomet. Chem.* **1992**, *428*, C44. (b) Noth, H.; Fluck, E. *Z. Naturforsch.* **1984**, *37b*, 744.

(28) Ellermann, J.; Knoch, F. A.; Meier, K. J. *Z. Naturforsch.* **1991**, *46B*, 1699.

(29) Kuang, S.; Zhang, L.; Zhang, Z.; Wu, B.; Mak, T. C. W. *Inorg. Chim. Acta* **1999**, *284*, 278.

(30) Shieh, S. J.; Li, D.; Peng, S. M.; Che, C. M. *J. Chem. Soc., Dalton Trans.* **1993**, 195.

(31) Bensch, W.; Prelati, M.; Ludwig, W. *J. Chem. Soc., Chem. Commun.* **1986**, 1722.

(32) Balakrishna, M. S.; Krishnamurthy, S. S.; Murugavel, R.; Mathews, I. I.; Nethaji, M. *J. Chem. Soc., Dalton Trans.* **1993**, 477.

(33) Kirss, R. V.; Eisenberg, R. *Inorg. Chem.* **1989**, *28*, 3372.

(34) Manojlovic-Muir, L.; Muir, K. W.; Grossel, M. C.; Brown, M. P.; Nelson, C. D.; Yavari, A.; Kallas, E.; Moulding, R. P.; Seddon, K. R. *J. Chem. Soc., Dalton Trans.* **1986**, 1955.

Table 5. Selected Bond Angles and Lengths for $\text{Ag}_2(\text{dppa})_3\text{BF}_4$

Bond Lengths, Å			
Ag(1)···Ag(2)	2.812(1)	P(1)–N(1)	1.691(10)
Ag(1)–P(1)	2.528(3)	P(2)–N(2)	1.688(10)
Ag(1)–P(2)	2.467(3)	P(3)–N(3)	1.676(9)
Ag(1)–P(3)	2.482(3)	P(4)–N(1)	1.705(10)
Ag(2)–P(4)	2.522(3)	P(5)–N(2)	1.695(10)
Ag(2)–P(5)	2.509(3)	P(6)–N(3)	1.725(9)
Ag(2)–P(6)	2.497(3)		
Bond Angles, deg			
Ag(2)–Ag(1)–P(1)	87.2(1)	P(5)–Ag(2)–P(6)	123.5(1)
Ag(2)–Ag(1)–P(2)	92.6(1)	P(1)–N(1)–P(4)	123.0(6)
Ag(2)–Ag(1)–P(3)	93.0(1)	P(2)–N(2)–P(5)	125.1(6)
P(1)–Ag(1)–P(2)	123.3(1)	P(3)–N(3)–P(6)	121.8(5)
P(1)–Ag(1)–P(3)	109.6(1)	Ag(1)–P(1)–N(1)	115.7(4)
P(2)–Ag(1)–P(3)	127.1(1)	Ag(1)–P(2)–N(2)	112.3(3)
Ag(1)–Ag(2)–P(4)	93.9(1)	Ag(1)–P(3)–N(3)	112.0(3)
Ag(1)–Ag(2)–P(5)	88.4(1)	Ag(2)–P(4)–N(1)	111.9(4)
Ag(1)–Ag(2)–P(6)	85.9(1)	Ag(2)–P(5)–N(2)	113.9(4)
P(4)–Ag(2)–P(5)	121.0(1)	Ag(2)–P(6)–N(3)	112.9(4)
P(4)–Ag(2)–P(6)	115.5(1)		

the mononuclear silver–monodentate phosphine complexes $\text{Ag}(\text{PPh}_3)_3\text{BF}_4$ ³⁵ and $[\text{Ag}\{\text{PPh}_2(\text{C}_5\text{H}_9)\}_3](\text{BF}_4)$ ³⁶ in which the net $\text{Ag}–\text{F}–\text{BF}_3$ interaction was described as somewhat weaker than the weak $\text{Cu}–\text{F}–\text{BF}_3$ coordination observed in $\text{Cu}(\text{PPh}_3)_3–\text{BF}_4$. The $\text{P}–\text{N}–\text{P}$ angles of the coordinated ligands range from 121.8(5) to 125.1(6)°, averaging 123.3°. This slight deviation from that found for the free ligand (118.9°)²⁸ and the ideal for sp^2 -hybridized nitrogen suggests minimal strain due to some $\text{Ag}\cdots\text{Ag}$ repulsive interaction. The $\text{Ag}–\text{P}–\text{N}$ angles range from 111.9(4) to 115.7(4)°, averaging 113.1°. This was close to that expected for phosphorus in a tetrahedral environment and points to the lack of strain. The analogous $\text{Ag}–\text{P}–\text{C}$ angle for $[\text{Ag}_2(\mu\text{-dppm})_3]^{2+}$ is 111.5°.²¹

The $\text{Ag}–\text{P}$ bond lengths (Table 5) vary from 2.467(3) to 2.528(3) Å. The average $\text{Ag}–\text{P}$ bond lengths for each silver are 2.492 and 2.482 Å, slightly longer than the 2.482 Å in $[\text{Ag}_2(\mu\text{-dppm})_3]^{2+}$.²¹ These bond lengths are slightly shorter though comparable to the average $\text{Ag}–\text{P}$ length of 2.54 Å found in $\text{Ag}(\text{PPh}_3)_3\text{BF}_4$ ³⁵ and 2.545 Å found in the $[\text{Ag}\{\text{PPh}_2(\text{C}_5\text{H}_9)\}_3]^+$ cation.³⁶ The average $\text{Ag}–\text{P}$ distance observed in the $[\text{Ag}_2(\text{dppa})_3]^{2+}$ was shorter than the expected $\text{Ag}–\text{P}$ bond length of 2.62 Å for a purely σ -bond, this indicating some $\text{d}\pi–\sigma^*$ interaction between silver and phosphorus as was observed in the $[\text{Ag}\{\text{PPh}_2(\text{C}_5\text{H}_9)\}_3]^+$ cation.³⁶

An average $\text{P}–\text{N}$ bond length of 1.697 Å is observed in the $[\text{Ag}_2(\mu\text{-dppa})_3]^{2+}$ complex cation, indistinguishable from the 1.692 Å found in the free ligand,²⁸ and is somewhat shorter than the accepted 1.77–1.80 Å for the purely $\text{P}–\text{N}$ σ -bond. This once again is indicative of some $\text{d}\pi–\text{p}\pi$ interaction between the phosphorus and nitrogen.

The $\text{Ag}\cdots\text{Ag}$ separation of 2.812(1) Å for $[\text{Ag}_2(\mu\text{-dppa})_3]^{2+}$ is virtually that found in metallic silver, i.e., 2.889 Å, much shorter than twice the van der Waals radius, 3.40 Å,³⁷ but lies within the range of reported distances for binuclear $\text{Ag}(\text{I})$ complexes reported in the literature.^{20,38} This separation is shorter than that found in the dinuclear doubly bridged $\text{Ag}_2(\mu\text{-dppm})_2$ and $\text{Ag}_2(\mu\text{-dmpm})_2$ core complexes and the

2.987 Å²¹ reported for $[\text{Ag}_2(\mu\text{-dppm})_3]^{2+}$. We thus have here the shortest reported $\text{Ag}\cdots\text{Ag}$ distance in these binuclear bisphosphine-bridged complexes. However, this intermetallic distance is longer than in some of the binuclear silver complexes bridged by N -donor ligands. A contributing factor to the $\text{Ag}\cdots\text{Ag}$ separation in $[\text{Ag}_2(\mu\text{-dppa})_3]^{2+}$ being shorter than in $[\text{Ag}_2(\mu\text{-dppm})_3]^{2+}$ despite the latter ligand having a smaller $\text{P}–\text{X}–\text{P}$, where $\text{X} = \text{N}$ (dppa) or C (dppm) in the complexes, is the nonbonded $\text{P}\cdots\text{P}$ distance. Using geometry, we estimate the $\text{P}\cdots\text{P}$ distances in the complexes to be 2.987 and 3.050 Å for $[\text{Ag}_2(\mu\text{-dppa})_3]^{2+}$ and $[\text{Ag}_2(\mu\text{-dppm})_3]^{2+}$, respectively. There is no $\text{Ag}–\text{F}$ contact less than 4 Å; one was 4.49 Å to $\text{Ag}(2)$ and another just over 5 Å to $\text{Ag}(1)$.

Conclusions

This work has addressed the relation between ligand to metal stoichiometry in solution and the ³¹P NMR $\text{Ag}–\text{P}$ coupling constant, hence the coordination number of the $\text{Ag}(\text{I})$ and the effect on coordination behavior of methylating the backbone in these bisphosphinoamines. ESMS at low sampling cone voltages reinforced the ³¹P NMR structural assignments. Dppa formed one-, two-, and three-coordinate complexes, while dppma formed one-, two-, and four-coordinate complexes, observations made for dppm and dppe, respectively. The maximum coordination number of $\text{Ag}(\text{I})$ was three or four, and none of the ligands showed both. The methylation at the bridging N is clearly seen to effect cyclization, here observed as the formation of the stable bis-chelated $[\text{Ag}(\mu\text{-P}\sim\text{P})_2]^+$ with dppma in solution, a complex not formed with dppa. This Thorpe–Ingold effect on the nitrogen, i.e., the smaller $\text{P}–\text{N}–\text{P}$ bond angle obtained by alkylation of nitrogen, results in favored formation of a four-membered ring, a ring size well-documented to be highly strained. This phenomenon may have practical applications where the variation of ring size causes changes in a desired property and the ring size of four is required.

The manxane-like solid-state structure of $[\text{Ag}_2(\text{dppa})_3]^{2+}$ was indeed that proposed independently by the Peringer¹⁹ and Dean²² groups for the dppm and dmpm analogues in solution and determined by Mak and co-workers²¹ for dppm in the solid state. The $[\text{Ag}_2(\text{dppa})_3]^{2+}$ here has the shortest reported $\text{Ag}\cdots\text{Ag}$ separation for a binuclear silver(I) bisphosphine bridged complex.

Experimental Section

Materials. Silver(I) tetrafluoroborate and dppma were synthesized. Dppa was obtained from Hokko Chemical (Japan) and used as received. Heptamethyldisilazane and chlorodiphenylphosphine were purchased from Aldrich Chemical Co., Inc. Microanalyses were performed by Atlantic Microlab, Inc., Atlanta, GA.

Physical Methods. Proton NMR spectra were recorded on a Bruker AC 250 multinuclear spectrometer operating at 250 MHz. The ³¹P NMR spectra were recorded on a Bruker AC 250 multinuclear spectrometer operating at 101 MHz and (for variable-

(35) Camalli, M.; Caruso, F. *Inorg. Chim. Acta* **1987**, *127*, 209.

(36) Baiada, A.; Jardine, F. H.; Willett, R. D. *Inorg. Chem.* **1990**, *29*, 4805.

(37) Bondi, A. J. *Phys. Chem.* **1964**, *68*, 441.

(38) (a) Karsch, H. H.; Schubert, U. Z. *Naturforsch.* **1982**, *37b*, 186. (b) Cotton, F. A.; Feng, X.; Matusz, M.; Poli, R. *J. Am. Chem. Soc.* **1988**, *110*, 7077. (c) Munakata, M.; Maekawa, M.; Kitagawa, S.; Adachi, M.; Masuda, H. *Inorg. Chim. Acta* **1990**, *167*, 181. (d) Fenske, D.; Baum, G.; Zinn, A.; Dehnicke, K. Z. *Naturforsch.* **1990**, *45B*, 1273.

temperature studies) a Bruker AM 400 multinuclear spectrometer operating at 162 MHz. The internal standard for ¹H was tetramethylsilane (TMS); the external standard for ³¹P spectra was 85% H₃PO₄. Chemical shifts (δ) were reported in parts per million (ppm) with peaks downfield of the standard given positive values. CDCl₃ and acetone-*d*₆ were used as internal lock solvents. Spectral simulations for [Ag₂(dppa)₂]²⁺ and [Ag₂(dppma)₂]²⁺ used the PANIC³⁹ program PANNICAL using the X part of the statistical sum of the AA'X₂X'₂' spin systems for the ¹⁰⁷Ag–¹⁰⁷Ag, ¹⁰⁷Ag–¹⁰⁹Ag, and ¹⁰⁹Ag–¹⁰⁹Ag combinations in a manner reported previously.^{18b,40} The simulated spectra were not optimized due to the inability of the program to handle spin systems of such complexity, but changing the calculated coupling constants led to dramatic changes in the calculated spectrum.

Electrospray mass spectra were recorded on a VG Trio 2000 quadrupole mass spectrometer with a water/acetonitrile (50:50) mobile phase. Calculations for assignments of peaks were based on ¹⁰⁷Ag, ¹¹B, ¹²C, ¹⁹F, ¹H, ¹⁴N, ¹⁶O, and ³¹P.

Crystal structure determination was performed on a Nicolet R3m/V diffractometer.

Preparation of Silver(I) Tetrafluoroborate, AgBF₄. In a centrifuge tube 1.58 g (8.63 mmol) of 48% aqueous HBF₄ was added to 1.00 g (4.31 mmol) of Ag₂O. The black silver oxide dissolved with effervescence. The tube was centrifuged and the clear colorless supernatant transferred to a 25 mL round-bottomed flask. A portion of methanol was added and the water/methanol mixture removed by vacuum. The white product was dissolved repeatedly in acetone, and the solvent was removed in vacuo. AgBF₄, a white solid that is light- and moisture-sensitive, was then dissolved in acetone or diethyl ether to ease its handling and the silver content determined by titration with standard ammonium thiocyanate solution with Fe(III) indicator.⁴¹ The silver(I) solution was stored in the dark.

Preparation of Bis(diphenylphosphino)methylamine. Hep-tamethylidisilazane (6.3 mL, 0.030 mol) was placed in a 500 mL round-bottomed flask and to this was added 20 mL of hexane. Chlorodiphenylphosphine (11.0 mL, 0.060 mol) was added to the flask followed by another 30 mL of hexane. The flask was incorporated into a simple distillation apparatus and the side product chlorotrimethylsilane (bp 57 °C) distilled off. The thick brown oil remaining in the boiling flask was dissolved in hot toluene (100 mL) with stirring and filtered while hot to give a clear orange-yellow solution. The solvent was reduced to about a third by rotary evaporation, resulting in a cloudy solution from which the white crystalline product precipitated on standing at 0 °C overnight. Yield: 5.3 g, 44%. δ(³¹P): 73.5. δ(¹H): 7.35 (m), 2.40 (t). Anal. Calcd (found): C, 75.17 (74.88); H, 5.82 (5.96); N, 3.51 (3.55). Mp: 112 °C.

Synthesis of Compounds. All of the compounds reported here are hygroscopic.

(a) [Ag₂(dppa)₂](BF₄)₂. A solution of dppa (0.385 g, 1.00 mmol) dissolved in 10.0 mL of methylene chloride was added to a solution of 5.00 mL of 0.200 M AgBF₄ in acetone. The solution was stirred for 15 min after which 5.0 mL of hexane was added, turning the clear solution cloudy. The solvent was removed in vacuo to give a white crystalline solid (0.42 g, 72% yield). δ(³¹P): 63.5(d) (¹J(¹⁰⁷-Ag–³¹P), 524 Hz). Calcd coupling constants: ¹J(¹⁰⁷Ag–P), 529 Hz; ¹J(¹⁰⁹Ag–P), 610 Hz; ³J(¹⁰⁷Ag–P), ³J(¹⁰⁹Ag–P), ²J(P~P), 183

Hz. Anal. Calcd (found): C, 49.69 (49.34); H, 3.66 (4.02); N, 2.42 (2.33). Mp: 157 °C, dec.

The following were synthesized as above with the appropriate molar ratios of silver(I) and ligand.

(b) [Ag₂(dppa)₃](BF₄)₂·2H₂O. Yield: 78%. δ(³¹P): 56.5(d) (¹J(¹⁰⁷Ag–³¹P), 350 Hz). Crystals suitable for X-ray crystallography were grown in methylene chloride. Anal. Calcd (found): C, 54.68 (54.84); H, 4.27 (4.36); N, 2.66 (2.61). Mp: 164 °C, dec.

(c) [Ag₂(dppma)₂](BF₄)₂. Yield: 60%. δ(³¹P): 81.5(d) (¹J(¹⁰⁷-Ag–³¹P), 524 Hz). Calcd coupling constants: ¹J(¹⁰⁷Ag–P), 529 Hz; ¹J(¹⁰⁹Ag–P), 610 Hz; ³J(¹⁰⁷Ag–P), ³J(¹⁰⁹Ag–P), ²J(P~P), 183 Hz. Anal. Calcd (found): C, 50.54 (51.74); H, 3.91 (4.31); N, 2.36 (2.98). Mp: 165 °C, dec.

(d) [Ag(dppma)₂](BF₄)₂·2H₂O. Yield: 78%. δ(³¹P): 89.4(d) (¹J(¹⁰⁷Ag–³¹P), 221 Hz). Anal. Calcd (found): C, 58.33 (58.22); H, 4.86 (4.86); N, 2.72 (2.58). Mp: 170 °C, dec.

Variable-Temperature ³¹P{¹H} NMR Studies. Appropriate molar amounts of ligand dppa or dppma dissolved in methylene chloride were added to an acetone solution of AgBF₄ (ca. 0.200 M) to yield mixtures with ligand concentration, C_L:Ag concentration, and C_M ratios ranging from 0.5 to 4.0. Solutions of solvent composition typically 59% methylene chloride, 40% CDCl₃, and 1% acetone were made up as (0.5–0.8) × 10⁻³ M on the basis of the expected complex. The expected complexes for the various C_L:C_M ratios were as follows; Ag₂(P~P)²⁺ for C_L:C_M = 0.5, Ag₂(P~P)₂²⁺ for C_L:C_M = 1.0, Ag₂(P~P)₂²⁺ for C_L:C_M = 1.25, Ag₂(P~P)₃²⁺ for C_L:C_M = 1.5, and Ag(P~P)₂⁺ for C_L:C_M ≥ 2.0. The solutions were run in situ at temperatures ranging from room temperature down to 213 K. Temperature calibration utilized methanol.

Electrospray Mass Spectrometry. The sample solutions were prepared by dissolving the appropriate molar ratios of AgBF₄ in acetone and the ligand in methylene chloride to give a 1.0 × 10⁻³ M solution based on expected complex. The solutions were then diluted 10 times with a 50:50 water/acetone mixture.

The electrospray mass spectra were recorded with a VG Trio 2000 quadrupole mass spectrometer with a water/acetonitrile (50:50) mobile phase. A Waters M-45 micro-LC syringe pump delivered the mobile phase into which sample solutions (1.0 × 10⁻⁴ M) were injected via a Rheodyne injector with a 10 μL sample loop, to the vaporization nozzle of the electrospray ion source at a flow of 3 μL min⁻¹. The analyte solutions were sprayed with nebulizing nitrogen gas from the tip of a stainless steel needle at 3.40 kV toward the sampling cone through a countercurrent flow of drying nitrogen. Sampling cone voltages were varied from 20 V (generally the minimum to maintain a stable ion spray) to 110 V. Generally at cone voltages of 50 V and above, collisions with solvent molecules within the ion source resulted in fragmentation of the silver–bisphosphine complex ions. Typically 8–12 signal-averaged spectra were sufficient to give mass spectra with good signal-to-noise ratios. The instrument was calibrated⁴² with poly(ethylene glycol) (300:600:1000 mixture) and horse heart myoglobin. Theoretical isotopic mass distributions were obtained with Isotope Pattern Calculator Version 1.6.6.⁴³

Instrument Settings. Needle voltage, 3.40 kV (2.80 kV for experimental isotopic mass distributions); repeller voltage, 0.38 kV (0.28 kV for experimental isotopic mass distributions); sampling

(39) Parameter adjustment by numerical iteration calculation.

(40) Bovey, F. A. *Nuclear Magnetic Resonance Spectroscopy*, 2nd ed.; Academic Press: San Diego, 1988; pp 179–85.

(41) Vogel, A. I. *Quantitative Inorganic Analysis*, 2nd ed.; Longman: London, 1951; pp 73–4 and 256–7.

(42) Fissions Instruments. *VG Trio-2000 Research Grade Mass Spectrometer, Users Guide*; VG Biotech: Altrincham, U.K., 1995.

(43) Arnold, L. *Isotope Pattern Calculator*, Version 1.6.6; Chemistry Department, University of Waikato: Hamilton, New Zealand, 2001.

cone voltage, 20–110 V; lens voltages, 63 and 12 V; electro spray source temperature, 60 °C; pressure, mass analyzer region, 3.0×10 mBar.

X-ray Crystallographic Structure Determination of [Ag₂(dppa)₃](BF₄)₂·H₂O. Crystals of X-ray crystallographic quality were obtained by the slow diffusion of hexane into a 0.20 M solution of [Ag₂(DPPA)₃](BF₄)₂ in methylene chloride. The crystal was mounted on the end of a glass fiber. The unit cell was determined by centering 25 reflections in the 2θ range of 17–28°.

Data were collected using the $2\theta/\theta$ scan technique and processed on a computer-controlled four-circle Nicolet R3m/V crystal diffractometer with Mo K α radiation. A summary of the crystallographic data is given in Table S-1 of the Supporting Information. Two reflections established as standards were checked routinely for deviations of positions and intensities after every 100 reflections. Lorentz and polarization corrections and empirical absorption corrections based on Ψ scans were performed. Systematic absences were consistent with space group *Cc* (no. 9) and *C2/c* (no. 15). Intensity statistics favored the noncentrosymmetric *Cc*.

Pseudosymmetry complicated the early efforts to solve the structure. A satisfactory starting point, derived in the space group *Cc* via direct methods,⁴⁴ consisted of the two Ag atoms and P atoms bound to one silver, chosen so that the Ag–Ag–P angles were all

ca. 90° and the P–Ag–P angles were all ca. 120°. All other non-hydrogen atoms were located in difference maps following refinement of this partial structure. The *x* and *z* coordinates of Ag(1) were fixed in order to define the origin. The phenyl rings were refined as rigid groups assuming *D*_{6h} symmetry with *d*_{C–C} = 1.395 Å and *d*_{C–H} = 0.960 Å. During the solution stage, one peak not connected with the cation or either anion was located. This was refined as the oxygen atom of a water molecule. All nongroup atoms were refined anisotropically. After this refinement, the structure was inverted to test the enantiomorph. The inverted structure refined to *R* = 0.0504 vs 0.0513 for the original choice; we therefore report the inverted structure. The hydrogens on N and O were not apparent in the final difference map and were not included in the final refinement; there may be one hydrogen bond between water and a F on one BF₄[–]. Again, small peaks suggestive of minor disorder appeared around F(1), F(2), F(3), and F(4); we did not attempt to refine this disorder.

Supporting Information Available: Table S-1, listing the structure determination summary; Table S-2, listing the atomic coordinates and equivalent isotropic displacement coefficients; Table S-3, listing the bond lengths; Table S-4, listing the bond angles; Table S-5, listing the anisotropic displacement coefficients; Table S-6, listing the H-atom coordinates and isotropic displacement coefficients. This material is available free of charge via the Internet at <http://pubs.acs.org>.

IC010661C

(44) All calculations employed: *SHELXTL PLUS VMS program package*, Release 4.11; Siemens Analytical X-ray Instruments, Inc.: Madison, WI, 1990. Based on SHELX (Sheldrick, G. M.).